

# Analysis of Heart Rate Variability Based on the Graph Method

V. A. Mashin

Novovoronezh Nuclear Power Station Personnel Training Center, Novovoronezh, Voronezh oblast, 396072 Russia

Received November 25, 2000

**Abstract**—A method of analysis of heart rate variability based on the graph theory principle was suggested. The main parameters of the heart rate graph structure were determined and analyzed using models of harmonic oscillations, white noise, and various functional tests (including controllable respiration and mental load). The efficiency of the use of parameters of the heart rate graph for diagnosing some functional states was considered. A correlation of the parameters of the heart rate graph structure with the frequency characteristics of heart rate variability was studied. A general model of changes in the heart rate graph structure parameters at different levels of mental activity was constructed in terms of entropy changes.

Difficult problems associated with informal interpretation of spectral analysis parameters of heart rate variability (HRV) [1] gave rise to a significant increase in the number of studies, in which the central role is played by the methods of nonlinear dynamics. These methods are used for determining the degree of chaotic character (uncertainty) of cardiac rhythm in different functional states [2–6]. Calculation of the maximum Lyapunov exponential index is the most common method of detection of chaotic dynamics of complex systems. The algorithms of the calculation of this value fall into two main classes. The algorithms of the first class implement the method of direct evaluation. This method is most frequently used in physiological research. It was shown in [7] that this method proved to be effective only in case of a sufficiently large sample, preliminary noise filtration, and in the absence of stochastic outburst in the system. The second class is based on the Jacobean method. It was tested using simulation and biological data [8]. This method was found to be sufficiently effective both in large (2000 observations) and in small (380 observations) samples. Because this method is based on extensive use of neural networks, its significant disadvantage is high cost of computation. For example, the time of processing of a sample of 336 RR-intervals is 18 h and 24 min (initial calculation parameters:  $L = 1$ ,  $d = 6$ ,  $k = 6$ ; hardware requirements: Pentium-MX, 166 MHz, and 16 Mbytes RAM).

Methodological and technological obstacles to the detection of chaotic dynamics of complex system on the basis of calculation of the maximum Lyapunov exponential index challenged us to develop a simple and illustrative method of assessment of nonlinear dynamics of cardiac activity.

The goal of this work was to attract the attention of researchers of HRV to the method of construction and analysis of RR-interval graph developed in our group. This method includes assessment of the degree of cha-

otic character (uncertainty) of heart rate. This method was tested using models of harmonic oscillations and white noise as well as results of heart rate measurements in various functional states.

## SUBJECTS AND METHODS

The method of construction and analysis of RR-interval graph suggested in this work was tested using results of examination of personnel of the Novovoronezh Nuclear Power Station at the Psychophysiological Laboratory, Novovoronezh Training Center. The subjects were divided into four groups with different functional states (males, ten subjects per group): (1) apparently healthy subjects waiting for the beginning of the attention test (mean age (*Age*), 30.08 years; standard deviation (SD), 6.69); (2) subjects with mental strain induced by attention test (*Age*, 29.59; SD, 3.80); (3) subjects with neurotic overexcitation during waiting for the beginning of the attention test (*Age*, 34.16; SD, 7.26); (4) subjects with reduced functional reserves during waiting for the beginning of the attention test (*Age*, 30.08; SD, 6.69). An increased level of neurotization as measured on a MMPI scale also characterized subjects of the third group. Asthenia symptoms were diagnosed in case of decreased working efficiency, reduced memory, and attention in psychophysiological tests and in case of complaint of enhanced fatigue.

A sample of 70 subjects (*Age*, 36.75; SD, 7.089) was taken for the correlation analysis of graph structure and HRV.

QRS-complexes were recorded, and RR-intervals were isolated from these complexes (sampling frequency, 500 Hz) using an RITMON-1 three-channel hardware-software system. Values of RR-intervals (duration of the cycle of cardiac contraction, ms) were stored as ASCII codes in the system memory for further computer processing. Electrocardiograms (ECG) were recorded in sitting subjects in the morning before psy-

chological tests (ECG record duration, 10 min) and during performing a computer version of the Schulte-Gorbov attention test. The MAVR-03 computer program developed at the Psychophysiological Laboratory, Novovoronezh Training Center, was used for editing  $RR$ -intervals (sliding samples of 256  $RR$ -intervals with a step of 10  $RR$ -intervals), plotting and structural analysis of heart rate graphs, and spectral analysis of variability.

A fast Fourier-transform algorithm and Hemming spectral window smoothing (moving mean window width, 5) were used to calculate characteristics of cardiac contraction spectrum. Trends were calculated and removed from temporal series using linear regression as described in [9]. The time invariance of the resulting samples was tested using mean and variance tests by the Spirman coefficient of ranking correlation [10]. The following HRV parameters were used in this work [11]:

(1)  $VLF$  ( $ms_2$ ) is the spectral power within the very low frequency range of cardiac contraction from 0.00 to 0.04 Hz (spectral range characteristic of contribution of cortico-limbic structures of brain to heart rate regulation [12]);

(2)  $LF$  ( $ms_2$ ) is the spectral power within the low frequency range of cardiac contraction from 0.04 to 0.15 Hz (spectral range typical mainly of activity of sympathetic segments of autonomic nervous system);

(3)  $HF$  ( $ms_2$ ) is the spectral power within the high frequency range of cardiac contraction from 0.15 to 0.40 Hz (spectral range characteristic of vagus activity);

(4)  $LF/HF$  ratio represents the balance between activities of sympathetic and parasympathetic segments of autonomic nervous system.

The frequency ranges of the spectral power of cardiac contraction ( $f_d$ ) are given for the mean value of  $RR$ -interval duration ( $RR_{mean}$ ) equal to 1.00 s. For the purpose of correction of boundaries of frequency ranges by  $RR_{mean}$  duration ( $f_{cor}$ ) and further calculation of HRV parameters, the following equation was used:  $f_{cor} = f_d RR_{mean}$ .

Consider the specific features of plotting and analysis of the heart rate graph in more detail. Usually, the heart rate is analyzed using a series of  $RR$ -intervals,  $RR_n$ , in which  $n$  is the number of cardiointervals ( $RR$ ) in sample. The graph of heart rate is defined analytically as a sequence of graph nodes (points of graph) with coordinates  $RR_n$  and  $RR_{n+1}$ :  $G = (RR_n, RR_{n+1})$ . Therefore, the total number of graph nodes (points of graph) is  $N - 1$ , where  $N$  is the sample size.

The values of  $RR$ -intervals used for describing graph were preliminarily rounded off accurate to 10 ms. This made the graphical representation of the heart rate graph more illustrative. Comparison between graph structure parameters calculated with different degree of accuracy of determination of  $RR$ -intervals revealed two specific consequences of rounding off. On the one hand, only a small volume of significant information is

lost as a result of rounding off. On the other hand, the use of rounded data makes it easier to diagnose some functional states.

The heart rate scattering diagram (scattergram) is widely used in medical practice. Scattergram is the curve of dependence of the scatter of variables  $RR_n$  and  $RR_{n+i}$ , where  $n$  is the number of  $RR$ -interval in sample and  $i$  is the lag-time ( $i = 1, 2, \dots, n - 1$ ). The scattergram was modified as follows to provide graphical presentation of the heart rate graph. All values of  $RR$ -intervals were preliminarily transformed into a new set using the following equation:

$$Z_n = W(RR_n - RR_{min})/BP,$$

where  $RR_{min}$  is the minimal value of  $RR$ -interval in sample,  $RD$  is the range of deviation ( $RD = RR_{max} - RR_{min}$ ), and  $W$  is the side of the square that inscribes standardized values of  $RR$  ( $Z_n$ ). The end values of  $Z_n$  are at the sides of the square ( $W = 400$  at display resolution of  $640 \times 480$ ).

At the next stage of the procedure, standardized values were used for plotting graph nodes with coordinates  $Z_n$  and  $Z_{n+1}$ . The resulting nodes were consequently connected to each other with lines (ribs) giving rise to a graph.

The heart rate graph structure can be schematically represented as a set of closed cyclic components (subgraphs). Closed cycle (initial and final nodes coincide with one another) passes through each rib and node of subgraph only once. Component ranks are distinguished in accordance with the cycle length (number of ribs). Isomorphism of graphs allows the shape of the components to be disregarded. The number of possible ranks of cyclic components is determined by the following equation:  $N_R = N - 2$ , where  $N$  is the sample size. The minimal and maximal ranks of cyclic component are 0 and  $N - 1$ , respectively. The component with zero rank includes two consecutive identical nodes (nodes with coinciding coordinates), and the number of ribs of the component is 0. Rank 1 is absent, because the requirement of closed cycle is not met. Possible number of components ( $M$ ) of rank  $R$  in graph with sample volume  $N$  is determined by the following equation:  $M_R = N - R - 1$ , where  $R = 1, 2, \dots, N_R$ . Corresponding value of accumulated frequency ( $F$ ) of components of rank  $R$  is calculated as:  $F_R = (C_R/M_R)$ , where  $C_R$  is the number of components of rank  $R$  in graph. It should be noted that graph components do not include closed cycles of lower rank.

The following parameters are calculated to analyze the heart rate graph structure:

$ND$  is the number of graph nodes (points);

$ND_S$  is the number of graph nodes per unit variance of  $RR$ -interval ( $S_{RR}^2$ ,  $ms^2$ );  $ND_S = ND/S_{RR}^2$  (graph node density in a square with side  $S_{RR}$ );

$SumF$  is the sum of accumulated frequencies over all ranks of cyclic graph components:  $SumF = \Sigma(F_R)$ ;

$N_{RG}$  is the number of ranks of cyclic components isolated in graph;

$N_{RG0}$  is the number of ranks of cyclic components with accumulated frequency higher than 0.01;

$M_F$  is the arithmetic mean of accumulated frequencies of graph:  $M_F = \text{Sum}F/N_{RG}$ ;

$F_{0n}$  is the percentage of accumulated frequency over the first rank of cyclic components in the total sum of accumulated frequencies of the whole graph:  $F_{0n} = 100F_0/\text{Sum}F$ ;

$F_{3n}$  is the sum percentage of accumulated frequency over the first three ranks of cyclic components ( $F_0$ ,  $F_2$ , and  $F_3$ ) in the total sum of accumulated frequencies of the whole graph:  $F_{3n} = 100(F_0 + F_2 + F_3)/\text{Sum}F$ ;

$F_{\max n}$  is the percentage of the maximal accumulated frequency of the total sum of accumulated frequencies of the whole graph:  $F_{\max n} = 100F_{\max}/\text{Sum}F$ ;

$R_{\max}$  is the rank of cyclic component of the graph with maximal accumulated frequency.

Harmonic oscillations (here and further the sample size was 256 values) were simulated using the following equation:

$$X_n = Am \cos(2\pi f) + Am \sin(2\pi f) + X_{\text{mean}},$$

where  $Am$  is the oscillation amplitude,  $f$  is the oscillation frequency, and  $X_{\text{mean}}$  is the arithmetic mean value (ms).

White noise (continuous in time signal of constant amplitude and uniform energy spectrum of equal frequency intervals) was generated using a sequence of pseudorandom numbers.

## RESULTS AND DISCUSSION

Graphs of  $Z_n$  values of samples simulated by the equation of harmonic oscillations are shown in Figs. 1A, 1B.

As a result of standardization, variation of neither the arithmetic mean value nor amplitude of harmonic oscillations modifies the size and shape of the graph. The frequency (period) of oscillations is of cardinal importance. Graphs of harmonic oscillations are composed of cyclic components of only one rank, which is equal to the period of oscillations (the number of identical nodes and ribs of each graph corresponds to the period ( $T$ ) of harmonic oscillations) and decreases upon increasing the oscillation frequency. (Integer values of oscillation period were chosen to provide easy-to-grasp presentation). Accumulated frequency of rank 1 components  $T(F_T)$  is equal to 1.0. The graphs have the shape of closed orbits (stability by Lyapunov), the orbit trajectory being dependent on the oscillation frequency. The lower is oscillation frequency (Fig. 1A), the closer is the orbit trajectory to the square diagonal. Conversely, the higher is oscillation frequency (Fig. 1B), the farther is the orbit trajectory to the square diagonal.

Heart rate graphs corresponding to controllable respiration test (respiration rate, 6 cycles per min; 0.1 Hz) are shown in Figs. 2A, 2B. In case of simulation of harmonic oscillations, the whole process is strictly determined and the accumulated frequency corresponds to components of only one rank (integer values of oscillation period). The period and amplitude of respiratory cycles mean value of heart rate, and exhalation/inhalation ratio may vary under conditions of controllable respiration test. This gives rise to a considerable diversity of cyclic components of heart rate graph and necessary use of probabilistic methods in graph analysis.

Graphs of white noise models are shown in Figs. 1C and 1D. The heart rate graphs corresponding to the state of deep relaxation (autotraining practice) and mental strain (Schulte-Gorbov attention test, level 3) are shown in Figs. 2C and 2D, respectively. To compare with the actual cardiac rhythm, white noise was simulated with the same values of  $S$  and  $X_{\text{mean}}$  as in states of mental strain and deep relaxation.

Very large number of nodes is typical of both high-amplitude white noise (Fig. 1C) and deep relaxation (Fig. 2C). However, in case of white noise, graph nodes are uniformly distributed over the square area, whereas the relaxed state graph is spindle-shaped and nodes are concentrated near its diagonal, which can be regarded as evidence of conservation of diverse wave periodicity of cardiac rhythm. It should be noted that low-amplitude white noise graph (Fig. 1D) is remarkably similar to the heart rate graph in the state of mental strain (Fig. 2D). The two types of graphs have equal number of nodes and similar structure. To reveal fine features of difference between these graphs, let us consider the main parameters of heart rate graph in more detail.

The values of structural parameters of graphs shown in Figs. 1 and 2 are summarized in Table 1.

As noted above, the parameter of the number of nodes ( $ND$ ) in case of harmonic oscillations corresponds to the sole rank of graph components ( $R_{\max}$ ) and is equal to the oscillation period (in case of integer period). The frequency accumulated over the sole rank of components is maximal and equal to 1.0. An increase in the frequency of harmonic oscillations causes a decrease in the number of nodes (at invariable variance), thereby causing a decrease in the node density per unit variance. Decreased node density is also observed upon increasing the amplitude (or variance) of harmonic oscillations (signal frequency is invariable). It was shown in our experiments that changes in the mean values of oscillation parameters (signal amplitude and frequency are invariable) the node density per unit variance is maintained at a constant level.

In controllable respiration tests, the heart rate graph provides information about the sophisticated character of nonlinear dynamics of cardiac rhythm. As noted above, it is impossible to provide strict control of respiratory cycle period, mean level of heart rate, duration of inhalation and exhalation phases, depth of respiration,

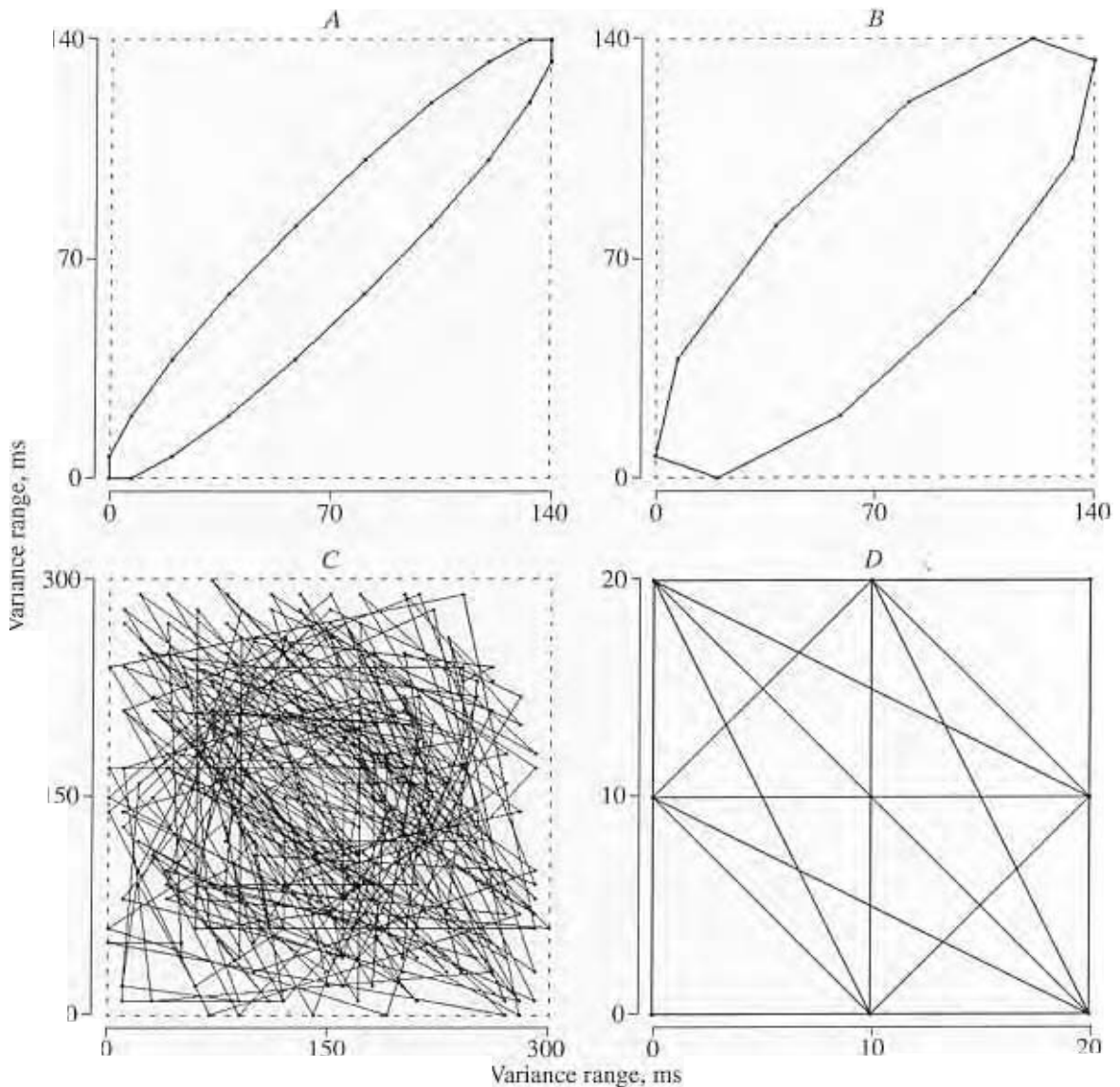


**Fig. 1.** Parameters of graphs of different signal models: (A) harmonic oscillations ( $f$  0.05,  $A_m$  0.05), (B) harmonic oscillations ( $f$  0.10,  $A_m$  0.05); (C) white noise (SD 0.085,  $X_{\text{mean}}$  1.120); (D) white noise (SD 0.006,  $X_{\text{mean}}$  0.380).

and human body resistance to oxygen saturation. The influence of these factors causes an increase in the number of observed component ranks (seven and six for graphs shown in Figs. 2A and 2B, respectively) and increases the graph shape diversity. As a result of significant increase in the number of nodes, graphs of controllable respiration tests have higher node density per variance unit than harmonic oscillations of the same frequency (Fig. 1B). On the other hand, parameters of relative accumulated frequency ( $\text{Sum}F$  and  $M_f$ ) in controllable respiration tests were significantly less than in strictly determined models of harmonic oscillations. Rank analysis of cyclic components of graph with maximal accumulated frequency can be used to determine

the period of waves observed in controllable respiration tests.

Values of the first three ranks of graph components ( $R$ ) with maximal accumulated frequency  $F_R$  are given in Table 2. It should be noted that graph 2A contains seven component ranks, the first three including about 71% of all graph components ( $F_{R_n}$  is the percentage of accumulated frequency of the  $R$ -rank components in the overall sum of accumulated frequencies of all component ranks). In case of graph 2B, corresponding values are six ranks and 70%. Because  $RR_{\text{mean}}$  is not equal to 1.0, the expected component rank ( $R_{\text{max}}$  10) differs from the actual values (13, 11). To calculate the actual period of respiratory waves, the obtained rank values (13 and 14 for graph 2A; 11 and 12 for graph 2B) should

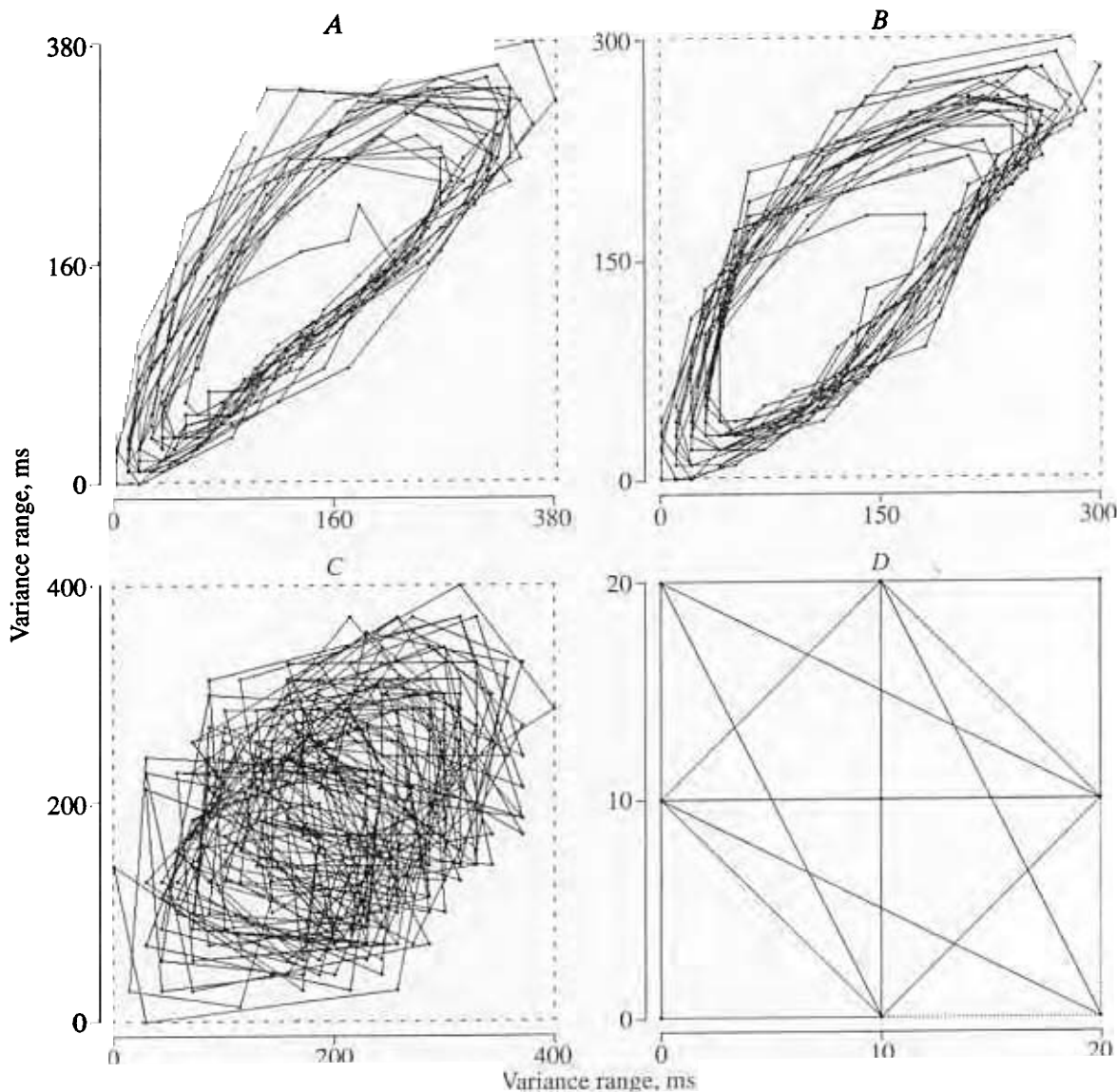


**Fig. 2.** Examples of heart rate graphs: (A) controllable respiration test (SD 0.107 s,  $X_{\text{mean}}$  0.750 s); (B) controllable respiration test (SD 0.087 s,  $X_{\text{mean}}$  0.880 s); (C) deep relaxation during autotraining practice (SD 0.085 s,  $X_{\text{mean}}$  1.120 s); (D) pronounced overstrain during attention test (SD 0.006 s,  $X_{\text{mean}}$  0.38 s).

be multiplied by the value of  $RR_{\text{mean}}$ . The ranks adjusted for heart rate value ( $R_{\text{cor}}$ ) allowed us to evaluate actual rate of controllable respiration. In the two samples this value ranged from 9.6 to 10.1 s. The mean rank value was 10.1 s, which was very close to set respiration period. It is interesting to note that frequencies of components of ranks 26 (graph 2A) and 23 (graph 2B) were increased. It may be concluded that after adjustment these values are equal to respiratory cycle period multiplied by two (19.4–20.1 s).

White noise models are characterized by more elaborate signal structure and complicated dynamics of parameters than harmonic oscillations. According to our findings, increase in the value of SD (or noise amplitude) is accompanied by logarithmic increase in

the number of nodes and exponential decrease in the node density per unit variance (variance increase is significantly larger than increase in the number of nodes). Mean accumulated frequency of components ( $M_F$ ) and their sum (SumF) are inversely proportional to the value of SD (or noise amplitude). This gives rise to gradual leveling of accumulated frequency values over all component ranks (parameter  $N_{RG0}$  tends to zero). In case of low-amplitude noise (Fig. 1D, SD 0.006), the main fraction of accumulated frequency (88%) falls within the first three ranks of graph components. The fraction of ranks of cyclic components with accumulated frequency larger than 0.01 ( $N_{RG0}$ ) approaches the total number of ranks of graph components ( $N_{RG}$ ). If the mean value of the signal is varied against the back-

**Table 1.** Parameters of graph structure for different models of signal (Fig. 1) and heart rate (Fig. 2)

Graph	$ND$	$ND_S \times 10^{-3}$	$SumF$	$N_{RG}$	$N_{RG0}$	$M_F$	$F_{0n}$	$F_{3n}$	$F_{maxn}$	$R_{max}$	$RR_{mean}$	$S_{RR}$
Fig. 1A	20	7.90	1.000	1	1	1.000	0	0	100	20	1.00	0.050
Fig. 1B	10	3.97	1.000	1	1	1.000	0	0	100	10	1.00	0.050
Fig. 1C	228	31.40	0.025	6	0	0.004	0	16	18	18	1.12	0.085
Fig. 1D	9	290.44	0.375	4	4	0.094	64	90	64	1	0.38	0.006
Fig. 2A	177	15.55	0.083	7	4	0.012	5	5	30	13	0.75	0.107
Fig. 2B	160	20.93	0.054	6	2	0.009	15	15	31	11	0.88	0.087
Fig. 2C	217	29.85	0.045	7	1	0.007	0	0	36	7	1.12	0.085
Fig. 2D	9	290.52	0.561	4	4	0.142	70	96	70	1	0.38	0.006

ground of invariable noise amplitude, it is only the mean frequency accumulated over ranks of graph components that undergoes substantial changes. In this case, there is a positive linear correlation between  $M_F$  and changes in mean signal amplitude.

As noted above, there is a close similarity between low-amplitude white noise graph (Fig. 1D) and heart rate graph in the state of pronounced mental strain (Fig. 2D). In case of coincidence between the number of nodes, the node densities in the two cases are equal to one another ( $ND_S$ ) and percentage of  $F_{0n}$  and  $F_{3n}$  is very high (this shows that contribution of linear component to the process is dominant). Values of  $N_{RG0}$  approach the value of  $N_{RG}$ . The results of our study showed that low-amplitude white noise corresponds to lower values of  $SumF$  and  $M_F$  (influence of chaos on the process).

High-amplitude white noise (graph 1C, SD 0.085) and the state of deep relaxation (graph 2C, SD 0.085) are also very much similar to one another in the number of nodes (therefore, node density per unit variance). The fraction of ranks of cyclic components with accumulated frequency larger than 0.01 ( $N_{RG0}$ ) in these processes approaches zero level. However, like in case of low-amplitude white noise, random character of noise signal generation gives rise to chaotization of the process, thereby causing a decrease in the accumulated frequency parameters ( $SumF$ ,  $M_F$ , and  $F_{maxn}$ ).

Let us consider the heart rate graphs in different functional states in more detail (Fig. 3).

Parameters of heart rate graph structure (arithmetic mean and SD) in different functional states (FS) are given in Table 3. Logarithmic plot (ln) was used in some cases to reduce the degree of asymmetry of distribution of some parameters.

The Student's  $t$ -test for independent samples was used for comparing the mean values averaged over groups (the program package Statistica v. 5.1 for Windows was used). The results of statistical analysis are given in Table 4. (It should be noted that according to the results obtained by Box and Andersen, if the sizes of samples are equal to each other, the effect of variance

heterogeneity on the level of confidence of the Student's  $t$ -test could be regarded as negligible [13]).

According to the results of statistical analysis, the state of mental strain is characterized by a decrease in the number of graph nodes, an increase in the node density per unit variance, and an increase in the values of all parameters of accumulated frequency over component ranks ( $SumF$ ,  $M_F$ ,  $F_{0n}$ ,  $F_{3n}$ ,  $F_{maxn}$ ). On the other hand, the overall number of ranks of graph components ( $N_{RG}$ ) decreases and the fraction of ranks of cyclic components with accumulated frequency larger than 0.01 ( $N_{RG0}$ ) increases. Components with zero rank have the maximal frequency. The results of comparison with the first group (normal subjects) suggest that the degree of manifestation of changes in these parameters depend on the severity of mental strain. A significant decrease in the value of  $RR_{mean}$  should also be noted.

Similar dynamics of these parameters was observed in subjects with neurotic reactions (the highest degree of coincidence was between  $F_{0n}$ ,  $F_{maxn}$ , and  $R_{max}$ ). The main difference between the states of neurotic reactions and mental strain is that the former is characterized by virtually invariable graph node density (dysregulation by  $ND_S$ ). Such invariability is explained by high values of heart rate variance.

In subjects with asthenia, there was a paradoxical pattern typical of the state of mental strain. A significant decrease in the number of nodes was observed against the background of increase in the node density

**Table 2.** The maximal accumulated frequencies for the first three ranks of heart rate graph components (controllable respiration tests, Figs. 2A and 2B)

Graph	$R$	$F_R$	$F_{Rn}$	$R_{cor}$
Fig. 2A	13	0.025	30	9.7
	26	0.021	25	19.4
	14	0.013	16	10.5
Fig. 2B	11	0.016	31	9.6
	12	0.012	23	10.5
	23	0.009	16	20.1

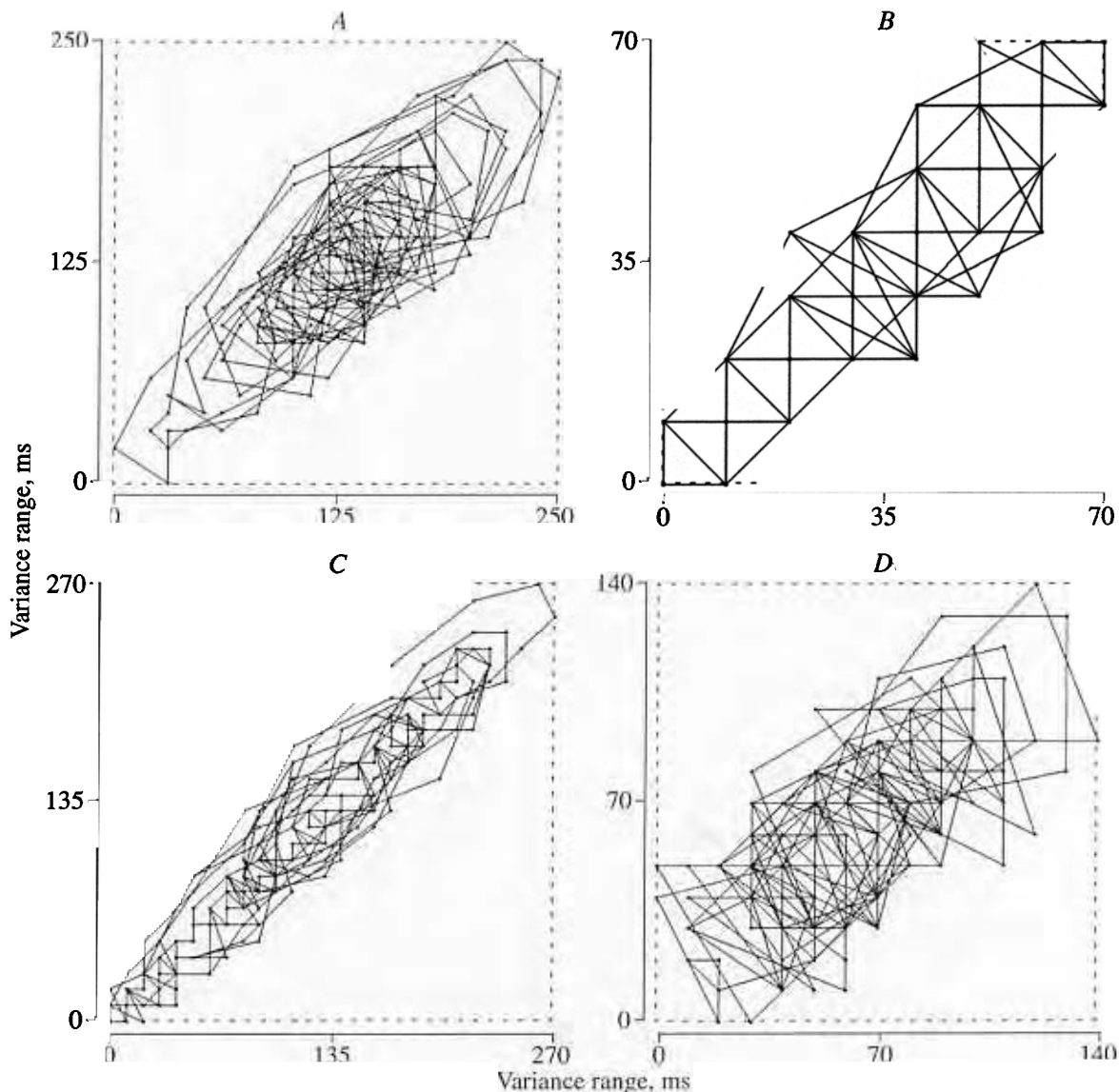


**Fig. 3.** Examples of heart rate graphs in different functional states: (A) normal state (waiting for the beginning of attention test); (B) mental strain during attention test; (C) neurotic excitation (waiting for the beginning of attention test); (D) reduced functional reserves (waiting for the beginning of attention test).

(up to the level typical of subjects with mental strain). This was also accompanied by a significant increase in the sum and mean frequencies of component ranks ( $\text{Sum}F$ ,  $M_F$ ) and fraction of ranks of cyclic components with accumulated frequency larger than 0.01 ( $N_{RG0}$ ). On the other hand, parameters  $F_{0n}$  and  $F_{3n}$  were increased to a lesser extent, the difference from the normal functional state (dysregulation by  $F_{0n}$  and  $F_{3n}$ ) being less pronounced in more quiet subjects. The lack of decrease in the value of  $RR_{\text{mean}}$  is the second important feature of difference.

Discriminant analysis was used at the next stage of the study to classify the states of interest according to heart rate graph parameters. The data obtained in all moving samples were used in this analysis: group 1,

403; group 2, 290; group 3, 718; and group 4, 153. First, three discriminant functions were found for determining the degree of deviation of the functional states of interest from normal level (contribution to the intergroup variance of parameters, 95–100%; confidence level by the Wilk  $\lambda$ -test,  $p = 0.0000$ ). Parameters  $ND$  and  $F_{3n}$  were found to be the most informative to distinguish between normal state and state of mental strain. Parameters  $\ln NDS$ ,  $ND$ , and  $F_{3n}$ , to distinguish between normal state and state of neurotic reaction; and parameters  $\ln NDS$ ,  $ND$ , and  $\text{Sum}F$ , to distinguish between normal state and state of asthenia. Two discriminant functions with total contribution to the intergroup variance of parameters of 96.48% and confidence level by the Wilk  $\lambda$ -test of  $p = 0.0000$  were determined at the

**Table 3.** Parameters of heart rate graph structure (mean values averaged over groups and SD) for different functional states (FS)

FS	ND	lnND <sub>S</sub>	lnSumF	N <sub>RG</sub>	N <sub>RG0</sub>	lnM <sub>F</sub>	F <sub>0n</sub>	F <sub>3n</sub>	F <sub>maxn</sub>	R <sub>max</sub>	RR <sub>mean</sub>	S <sub>RR</sub>
1	169.7	10.75	-2.78	9.58	1.53	-5.02	8.5	17.0	23.1	8.95	0.94	0.062
	33.61	0.370	0.335	1.50	1.22	0.257	7.29	11.73	5.30	4.99	0.084	0.017
2	37.0	11.69	-1.11	6.17	3.93	-2.88	67.1	86.7	67.1	1.00	0.53	0.017
	15.98	0.232	0.368	1.93	1.03	0.696	15.71	13.61	15.71	0.00	0.040	0.005
3	115.8	10.49	-1.90	8.44	3.01	-4.03	56.6	70.9	56.7	1.14	0.64	0.058
	30.41	0.397	0.308	1.03	0.58	0.379	14.83	14.43	14.66	0.30	0.056	0.019
4	81.8	11.69	-1.98	9.69	4.41	-4.23	18.4	38.8	33.9	2.89	0.98	0.026
	13.41	0.204	0.155	1.54	0.92	0.240	12.76	16.37	5.19	1.28	0.082	0.005

**Table 4.** Values of Student's *t*-test for comparing mean values in independent samples

Parameter	Groups compared					
	1-2	1-3	1-4	2-3	2-4	3-4
ND	11.28***	3.76**	7.68***	-7.26***	-6.80***	3.23**
lnND <sub>S</sub>	-6.77***	1.50	-7.02***	8.21***	-0.03	-8.47***
lnSumF	-10.60***	-6.07***	-6.87***	5.23***	6.86***	0.66
N <sub>RG</sub>	4.41***	1.98	-0.15	-3.28**	-4.50***	-2.13*
N <sub>RG0</sub>	-4.76***	-3.45**	-5.95***	2.48*	-1.10	-4.08***
lnM <sub>F</sub>	-9.14***	-6.86***	-7.10***	4.59***	5.82***	1.45
F <sub>0n</sub>	-10.70***	-9.20***	-2.14*	1.54	7.61***	6.16***
F <sub>3n</sub>	-12.26***	-9.16***	-3.42**	2.51*	7.11***	4.65***
F <sub>maxn</sub>	-8.39***	-6.81***	-4.60***	1.54	6.35***	4.63***
R <sub>max</sub>	5.04***	4.94***	3.72**	-1.50	-4.66***	-4.19***
RR <sub>mean</sub>	13.81***	9.32***	-1.23	-5.00***	-15.62***	-10.91***
S <sub>RR</sub>	7.93***	0.41	6.38***	-6.46***	-4.13***	5.09***
Age	-1.13	0.27	-1.95	1.15	-1.04	-1.91

Note: *p* is the level of statistical significance of *t*-test. \**p* < 0.05, \*\**p* < 0.01, \*\*\**p* < 0.001

final stage of analysis. These functions allow the subjects tested by the results of heart rate graph analysis to be attributed to four classes of functional states. Parameters  $F_{0n}$  and  $RR_{mean}$  were additionally included in the discriminant functions to increase their sensitivity.

Correlation of graph parameters with temporal and frequency characteristics of HRV is of particular interest. The data averaged over moving samples obtained in 70 subjects were subjected to correlation analysis. The heart rate was measured before testing. The logarithmic plot was used to reduce the degree of asymmetry of distribution of spectral analysis parameters. Pearson correlation coefficients between graph parameters and characteristics of HRV are given in Table 5.

Analysis of the correlation matrix demonstrated a negative correlation of parameters of accumulated frequencies of ranks of graph components (SumF, M<sub>F</sub>, F<sub>0n</sub>, and F<sub>3n</sub>) with spectral power of cardiac contraction upon increasing the frequency range (from VLF to HF).

An opposite pattern was typical of graph node density: negative correlation with spectral power parameters increases upon decreasing the frequency range (from HF to VLF). The use of the correlation matrix in factor analysis (method of main components and Varimax Normalized rotation) supported the conclusions drawn above. Two leading factors (with the total accumulated contribution to variance of parameters of 88.32%) were isolated. The first factor included frequency parameters of ranks of graph components and spectral power of cardiac contraction within the HF range (the higher were parameters of accumulated frequencies, the lower was the HF spectral power). The second factor included ND<sub>S</sub> and spectral power within the VLF- and LF ranges (the higher was graph node density, the lower was the VLF and LF spectral power).

An additional goal of this study was to analyze the correlation of the graph node number (ND) with the entropy of node distribution  $H = -\sum pND_i \times \ln(pND_i)$ ,

Table 5. Results of correlation analysis of graph structure and heart rate variability

	$ND$	$\ln ND_S$	$\ln \text{Sum} F$	$\ln M_F$	$F_{0n}$	$F_{3n}$	$RR_{\text{mean}}$	$S_{RR}$	$\ln VLF$	$\ln LF$	$\ln HF$
$\ln ND_S$	-0.80	×									
$\ln \text{Sum} F$	-0.94	0.69	×								
$\ln M_F$	-0.87	0.51	0.93	×							
$F_{0n}$	-0.59	0.20**	0.66	0.77	×						
$F_{3n}$	-0.68	0.28*	0.74	0.83	0.90	×					
$RR_{\text{mean}}$	0.57	-0.32	-0.58	-0.55	-0.72	-0.56	×				
$S_{RR}$	0.90	-0.96	-0.83	-0.66	-0.37	-0.45	0.45	×			
$\ln VLF$	0.77	-0.91	-0.61	-0.48	-0.24**	-0.28*	0.36	0.85	×		
$\ln LF$	0.76	-0.77	-0.73	-0.64	-0.21**	-0.33	0.19**	0.79	0.59	×	
$\ln HF$	0.88	-0.56	-0.87	-0.86	-0.77	-0.83	0.63	0.73	0.50	0.56	×
$\ln LF/HF$	-0.44	0.06**	0.46	0.52	0.76	0.73	-0.60	-0.24**	-0.12**	0.13**	-0.75

Note:  $p$  is the level of statistical significance of Pearson's correlation coefficient. \* $p > 0.01$ , \*\* $p > 0.05$ .

where  $pND_i$  is the probability of the node with coordinates  $i$ . It was found that the Pearson correlation coefficients between  $ND$  and  $H$  is 0.98. Because the coefficient of correlation between the graph node number and entropy of node distribution is large, it may be suggested that parameter  $ND$  is the measure of uncertainty of heart rate graph. In this case, the heart rate graph entropy should have the following main properties [14]:

(1) Among equiprobable distributions, the highest entropy is inherent in distributions with the largest number of possible values of random variable. Parameters of accumulated frequency over component ranks ( $\text{Sum} F$ ,  $M_F$ ,  $F_{0n}$ ,  $F_{3n}$ ) can be used as characteristics of the probability of distribution of graph nodes. In the state of deep relaxation, there is a decrease in these parameters and in the value of  $N_{\text{RGO}}$  (fraction of ranks with accumulated frequency larger than 0.01). The frequencies accumulated over ranks attain equiprobable character. In this case, the heart rate entropy increases with increasing the number of graph nodes.

(2) Among distributions with equal number of possible values, the highest entropy is inherent in distributions with equiprobable values. In the state of mental strain there is an increase in the absolute values of parameters of accumulated frequency over component ranks ( $\text{Sum} F$ ,  $M_F$ ,  $F_{0n}$ ,  $F_{3n}$ ) and pronounced dominance of accumulated frequencies of zero rank ( $F_{0n}$ ), i.e., an increase in the contribution of the linear component of the process. Opposite trends are typical of the state of relaxation. In this case, the heart rate entropy increases with decreasing the parameters of accumulated frequency over graph component ranks.

The results of this study are consistent with the conclusions of some researchers, who suggested that HRV is based on chaotic dynamics [2]. Within the framework of the white noise model, an increase in the noise amplitude is accompanied by an increase in the system entropy (chaos). Therefore, this process is accompa-

nied by an increase in the number of graph nodes and a decrease in the parameters of accumulated frequency. As noted above, similar processes are typical of the state of deep relaxation of healthy subjects.

It was shown in our experiments that parameter  $ND_S$  is also important for assessing heart rate parameters. Using correlation analysis it was found that this parameter primarily correlates with spectral power within the  $VLF$  range ( $r = -0.91$ ). It was suggested in one of our earlier works, devoted to analysis of heart rate variability during psychological relaxation after test-induced negative functional states [12], that spectral power in the  $VLF$  range may represent activity of the cortico-limbic systems, which becomes dominant in subjects with neurotic disorders. If this suggestion is true, parameter  $ND_S$  may represent activity of cortico-limbic structures of brain, which causes the phenomenon of dysregulation by  $ND_S$  observed in the state of neurotization.

According to the results of correlation and factor analysis, there is a close inverse correlation of parameters of frequency accumulated over ranks of graph components with spectral power characteristics in the  $HF$  range, which is closely associated with parasympathetic activity. It may be suggested that parasympathetic activity (absolute or relative) is reduced in the state of mental strain, thereby causing an increase in the frequency parameters of the heart rate graph and rise of accumulated frequencies of the first three ranks of graph components (stabilization effect, i.e., an increase in the linear component of the process). Such dynamics was observed during psychological testing. A frequency increase in ranks corresponding to the respiratory wave period can be observed at high activity of parasympathetic system (state of relaxation, asthenia).

In our experiments, there was a high correlation of the number of graph nodes with spectral power in the  $HF$  range of cardiac contraction ( $r = 0.88$ ). These data

are consistent with the results obtained by a group of physiologists from Jena University (Germany) [15]. These researchers showed that deterministic chaos and periodic components of heart rate variability are mediated mainly by vagus activity. Taking into account that  $ND$  is the measure of entropy (uncertainty, chaos), whereas spectral power within the  $HF$  range represents the effects of the parasympathetic system, the resulting high positive correlation between these parameters has a specific physiological sense.

To sum up the results considered above, the following model of changes in heart rate graph structure at different levels of mental activity of humans may be suggested. Solution to difficult test task causes an increase in the mental activity, which is accompanied by a decrease in the level of entropy (uncertainty, chaos) of heart rate signal distribution (decrease in the number of graph nodes). This shifts the balance of autonomic nervous system toward sympathetic activity (increase in the contribution of parameters of accumulated frequency over components of graph ranks, dominance of zero rank components, and increase in the heart rate). Chronic overstrain causes exhaustion of functional resources of human body. The HRV changes described above are observed in this case in the state of rest (asthenic processes). The heart rate is not increased, whereas the maximal frequency of components falls within the rank corresponding to the respiratory wave period. The last changes are determined by the level of parasympathetic activity (these changes may be absent in the state of deep exhaustion).

The level of entropy (uncertainty, chaos) of heart rate signal distribution gradually increases (increase in the number of graph nodes, frequency parameters of components are decreased and attain equiprobable values) upon deepening the state of relaxation. In the presence of a well-pronounced respiratory wave, there is an increase in the frequency of rank components corresponding to the respiratory wave period. If similar changes are observed in the state of active rest or during mental activities, pronounced disorders of heart rate automatism may be diagnosed. These disorders may cause heart rate regulation failure.

## CONCLUSION

The use of the graph method for analyzing models of harmonic oscillations allowed a correlation between the period of harmonic oscillations and rank of graph components with the maximal accumulated frequency ( $R_{max}$ ) to be found. Further analysis of heart rate graph in controllable respiration tests (respiration rate, 0.1 Hz) confirmed this suggestion. In further studies, I plan to analyze the correlation of the heart rate graph structure parameters with activity of different segments of autonomic nervous system in controllable respiration tests in more detail.

Comparative analysis of graphs of white noise models and heart rate graphs during mental tests revealed that low-amplitude white noise graph is similar to the heart rate graph in the state of mental strain (significant decrease in the number of graph nodes, increase in the node density, and very high percentage of  $F_{0n}$  and  $F_{3n}$ ). Parameters of high-amplitude white noise graph were found to be similar to parameters of the heart rate graph in the state of deep relaxation (high value of  $ND$ , low value of  $ND_s$ , and low values of parameters of accumulated frequency of component ranks). Further analysis revealed a high correlation between parameter  $ND$  and entropy of graph node distribution. This provided a basis to suggest that parameter  $ND$  is a measure of entropy (uncertainty) of heart rate graph. In this case, the higher is mental strain, the lower is entropy (chaotic dynamics) of heart rate. In contrast, the entropy (chaotic dynamics) of the heart rate in relaxed human body is increased. If two graphs have an equal number of nodes, the state of deeper relaxation corresponds to lower value of accumulated frequency of component ranks.

The use of the heart rate graph method for diagnosing various functional states (mental strain, neurotic reactions, and asthenia) provided information about statistically significant deviation of these states from normal state. This information can be obtained on the basis of graph structure parameters. Discriminant analysis was used to reveal the heart rate graph parameters providing the most valuable information for differential diagnosis of the functional states of interest. Further studies are expected to refine the discriminant functions and to extend the list of functional states.

Correlation and factor analyses of correlation of heart rate graph structure parameters with parameters of spectral analysis of heart rate variability showed that there was close correlation of the density of nodes ( $ND_s$ ) with spectral power in the  $VLF$  range (level of activity of cortico-limbic structures of brain) and frequency characteristics of graph components ( $SumF$ ,  $M_F$ ,  $F_{0n}$ ,  $F_{3n}$ ) with spectral power in the  $HF$  range (dominance of parasympathetic activity in the balance of autonomic nervous system). It is very important to note that the heart rate graph method proved to be more stable in analysis of nonstationary processes than spectral analysis. However, elucidation of this problem requires additional research.

The results of this study enabled us to put forward a model of changes in heart rate graph parameters at different levels of mental activity. This model is based on the concept of entropy (uncertainty). Further studies are planned to test the validity of the model.

## REFERENCES

1. Eckberg, D.L. Sympathovagal Balance, A., Critical Appraisal, *Circulation*, 1997, vol. 96, p. 3224.
2. Guzzetti, S., Signorini, M.G., Cogliati, C., *et al.*, Nonlinear Dynamics and Chaotic Indices in Heart Rate Vari-

- ability of Normal Subjects and Heart-Transplanted Patients, *Cardiovasc. Res.*, 1996, vol. 31, no. 3, p. 441.
3. Lombardi, F., Sandrone G., Mortara, A., *et al.*, Linear and Nonlinear Dynamics of Heart Rate Variability after Acute Myocardial Infarction with Normal and Reduced Left Ventricular Ejection Fraction, *Am. J. Cardiol.*, 1996, vol. 77, no. 15, p. 1283.
  4. Kagiya, S., Tsukashima, A., Abe, I., *et al.*, Chaos and Spectral Analyses of Heart Rate Variability during Head-up Tilting in Essential Hypertension, *J. Auton. Nerv. Syst.*, 1999, vol. 76, nos. 2–3, p. 153.
  5. Fortrat, J.O., Formet, C., Frutoso, J., and Gharib, C., Even Slight Movements Disturb Analysis of Cardiovascular Dynamics, *Am. J. Physiol.*, 1999, vol. 277, no. 1, pt. 2, p. 261.
  6. Yeragani, V.K., Jampala, V.C., Sobelowski, E., *et al.*, Effects of Paroxetine on Heart Period Variability in Patients with Panic Disorder: A Study of Holter ECG Records, *Neuropsychobiology*, 1999, vol. 40, no. 3, p. 124.
  7. Smith, R.L., Estimating Dimension in Noisy Chaotic Time Series, *Royal Statistical Society*, 1992, vol. 54, no. 2, p. 329.
  8. Nychka, D., Ellner, S., Gallant, R., and McCaffrey, D., Finding Chaos in Noisy Systems, *Royal Statistical Society*, 1992, vol. 54, no. 2, p. 399.
  9. *Spravochnik po prikladnoi statistike* (Handbook of Applied Statistics), Lloid, E., Lederman, W., and Tyurin, Yu.N., Eds., Moscow: Finansy Statistika, 1989, vol. 1.
  10. Candell, M.J., and Stewart, A., *Mnogomernyi statisticheskiy analiz i vremennye ryady* (Multidimensional Statistical Analysis and Time Series), Moscow: Nauka, 1976.
  11. Task Force of the European Society of Cardiology and the North American Society of Pacing and Electrophysiology. Heart Rate Variability. Standards of Measurements, Physiological Interpretation, and Clinical Use, *Circulation*, 1996, vol. 93, p. 1043.
  12. Mashin, V.A., and Mashina, M.N., Analysis of Heart Rate Variability in Negative Functional States during Psychological Relaxation Tests, *Fiziol. Chel.*, 2000, vol. 26, no. 4, p. 48.
  13. Glass, G., and Stanley, G., *Statisticheskie metody v pedagogike i psikhologii* (Statistical Methods in Pedagogy and Psychology), Moscow: Progress, 1976.
  14. Artem'eva, E.Yu., and Martynov, E.M., *Veroyatnostnye metody v psikhologii* (Probabilistic Methods in Psychology), Moscow: Mosk. Gos. Univ., 1975.
  15. Zwiener, U., Hoyer, D., Luthke B., *et al.*, Relations between Parameters of Spectral Power Densities and Deterministic Chaos of Heart-Rate Variability, *J. Auton. Nerv. Syst.*, 1996, vol. 57, no. 3, p. 132.